EPR study of vanadium (4 +) in the anatase and rutile phases of TiO_2

R. Gallay and J. J. van der Klink
Institut de Physique Expérimentale, Ecole Polytechnique Fédérale de Lausanne, PHB-Ecublens, CH-1015 Lausanne, Switzerland

J. Moser
Institut de Chimie Physique, Ecole Polytechnique Fédérale de Lausanne, CHB-Ecublens, CH-1015 Lausanne, Switzerland
(Received 21 April 1986)

We present cw and pulsed EPR experiments on V^{4+} in the rutile and anatase phases of TiO_2. For the rutile phase, the cw data confirm earlier results, but the relaxation data are different from those previously reported. No earlier results for V^{4+} in the unreduced pure anatase phase exist. We show that a simple point-charge model can be used to interpret the values of the g tensors, but that models considering only nearest neighbors will give erroneous results. We conclude that the observed V^{4+} is substitutional in the rutile, but interstitial in the anatase phase. We propose a relaxation mechanism through phonon-modulated hyperfine coupling to explain our T_1 data in the rutile phase.

I. INTRODUCTION

In this paper we will be concerned with the rutile and anatase phases of titanium dioxide. Rutile TiO_2 is an incipient ferroelectric wide-gap semiconductor.[1] Covalent bonding between the transition-metal d orbitals and oxygen p states is thought to enhance anisotropically the strong oxygen polarizability, and thus induce the (incipient) ferroelectric behavior. By reduction of stoichiometric rutile TiO_2, n-type semiconducting behavior is obtained,[2] probably involving the formation of Ti^{3+} ions or oxygen vacancies. Colloidal TiO_2 particles of both structures loaded with suitable catalysts are increasingly studied in light-induced water cleavage schemes;[3] here too the semiconducting nature of the carriers is believed to be important. Pure anatase single crystals cannot presently be grown in the laboratory, since up to a few percent of alumina is needed as a stabilizer[4] and most preparations of anatase powder yield a significant fraction of amorphous material. As a result, the anatase has been studied less thoroughly than the rutile phase.

We present new experimental cw and pulsed EPR data on V^{4+} in both phases. A critical discussion will be given of the relation of these data to earlier experiments and their interpretation. For the rutile phase we had two main reasons to take up this much-studied field again: on the one hand, the reported existence of a "direct-process" relaxation mechanism,[5] rather unexpected for a Kramers ion and which should be inhibited[6] in the fine powders[7] used in catalytic experiments; and on the other hand, the ligand field splitting[8,9] derived from earlier cw experimental data,[10,11] that does not show a level believed to be involved in a reported "Orbach process" relaxation,[5] nor is consistent with results of simple MO_6 ligand field theory (M = metal, O = ligand).[12] For the anatase phase, little earlier work exists and one of our interests was to observe the anatase-rutile structural transformation that occurs irreversibly when the material is heated to 700 °C.

The V^{4+} ion is isoelectronic with the Ti^{3+} defect created by reduction or by uv irradiation (in the presence of suitable hole scavengers[13]), but is much easier to identify in EPR because of its marked hyperfine interaction.

II. EXPERIMENTAL DETAILS

We have prepared ultrafine vanadium-doped TiO_2 powders by a procedure directly derived from that reported for the preparation of well-characterized colloidal TiO_2 sols.[7] $TiCl_4$ (Fluka, purissimum) was further purified by vacuum distillation (40 °C, 20 Torr) to yield a colorless liquid. The purified material (5 g) was slowly added to 200 ml of water at 0 °C containing a judicious amount of $VOSO_4 \cdot 5H_2O$ (Fluka, purum). The final pH was 0.5. The blue solution was subsequently dialyzed for 1 hour against a $VOSO_4$ solution of the same concentration and then in pure water until the pH of the sol reached ~ 2.7. During dialysis, the remarkable disappearance of the blue color, due to $[VO(H_2O)_4]^{2+}$ in solution, and the appearance of a yellowish transparent suspension indicate incorporation of V^{4+} ions in the TiO_2 matrix during its formation.

Precise determination of the TiO_2 content after dialysis was carried out as described previously.[14] Typically, the sol obtained contains about 10 g TiO_2 per l. Electron microscopy and quasielastic light-scattering[15] showed that it consisted of spherical particles of 100—200 Å diameter.

Finally, preparation of powdered samples was achieved by evaporating the sol at 40 °C under reduced pressure and repeated washing by water. The ultrafine aggregates of doped titanium dioxide consist of both the amorphous phase and anatase as shown by electron and x-ray diffraction. No trace of rutile nor any other phases could be detected. Conversion to the rutile form was carried out by heating the powdered samples in quartz crucibles for 14 hours at 700 °C in air.

Single crystals are only available in the rutile form. The crystals we used have been grown by Djévahirdjian Société Anonyme (CH-1870 Monthey, Switzerland) using

TABLE I. Lattice parameters (Å), 4(2) titanium-oxygen separations of equal length (Å), bond lengths (Å), EPR gyromagnetic, and hyperfine (10^{-4} cm^{-1}) tensorial principal values for V^{4+} in different hosts. Asterisk denotes interstitial site (1.964 for the substitutional site).

Type	TiO_2 Rutile	β-VO_2 Rutile	GeO_2 Rutile	RuO_2 Rutile	SnO_2 Rutile	TiO_2 Anatase
a (Å)	4.5929[a]	4.53[b]	4.395[b]	4.4919[c]	4.737[b]	3.785[a]
c (Å)	2.9591	2.869	2.852	3.1066	3.185	9.514
4 Ti-O (Å)	1.946	1.902	1.91	1.983	2.051	1.937
2 Ti-O (Å)	1.984	1.954	1.86	1.944	2.0565	2.804*
$\lvert A_x \rvert$ (10^{-4} cm^{-1})	31	27[d]	36.69[e]		21.1[f]	48
$\lvert A_y \rvert$ (10^{-4} cm^{-1})	44	45	37.54		41.8	48
$\lvert A_z \rvert$ (10^{-4} cm^{-1})	142	140	134.36		140.1	158
g_x	1.914	1.95	1.9213		1.939	1.96
g_y	1.912	1.95	1.9213		1.903	1.96
g_z	1.956	1.948	1.9632		1.943	1.932

[a]Reference 41.
[b]Reference 40.
[c]Reference 31.
[d]Reference 24.
[e]Reference 22.
[f]Reference 23.

the Verneuil technique. Nominally, the V^{4+} impurity content was 0.02 at. %. A part of this crystal has been ground in order to check the results found with the dispersed material prepared by us.

The cw ESR work has been carried out on an E-203 Varian spectrometer working at X band and on a homemade spectrometer working in power detection at K band. A homodyne X-band pulsed spectrometer has been used to study the spin-lattice relaxation. In this case, the output of a microwave sweep generator is amplified by a traveling wave tube before being fed into the resonator. The microwave power is pulsed with several PIN diode switches. A loop-gap resonator has been chosen because of its very high filling factor, moderate quality factor, and its small size.[16] The resonance frequency could be varied between 8 and 11 GHz. The temperature has been measured with a carbon-glass resistor mounted in the wall of the resonator's screen and by a thermocouple mounted in the wall of the cryostat.

The spin-lattice relaxation time T_1 is determined by recording the amplitude of a spin echo[17] following a $\pi/2$-τ-π sequence of pulses, with fixed τ, as a function of the time passed between and inversion π pulse and the $\pi/2$-τ-π sequence. The decay curves are digitized and stored in a computer. Multiple scans are performed in order to improve the signal-to-noise ratio of the recovery curve. The spin-lattice-relaxation curves in the experiments reported here cannot be fitted with single exponentials. We consider the initial fast decay to be due to cross relaxation, and determine the time T_1 from the tail of the recovery curve.

III. CRYSTAL-FIELD CALCULATIONS

The magnetic properties of V^{4+} in TiO_2 can be described by intermediate crystal-field theory: the spin-orbit and Zeeman interactions are of comparable magnitude and both are much smaller than the crystal-field interaction. We have used a simple point-charge model to calculate the orbital energy levels in the crystal field.[18] In such a model, the orbit of the $3d_1$ electron is not supposed to overlap with the point charges that represent the other ions in the crystal. The covalency that exists in the real crystal (as demonstrated by the existence of superhyperfine coupling with the two nearest Ti neighbors[19–21]) is empirically taken into account by allowing the radial averages $\langle r^2 \rangle$ and $\langle r^4 \rangle$ to be different from the free-ion values. They are adjusted to fit the experimental to the calculated values of the g tensor, and are expected to increase with increasing overlap. In the basis formed by the d-atomic orbitals, the cubic and tetragonal field operators are diagonal, but the orthorhombic field is not: it mixes the $d_{x^2-y^2}$ and $d_{3z^2-r^2}$ orbitals.

We have performed the necessary lattice sums on a desktop Hewlett-Packard 9816 computer. All ions were represented as point charges of charge 4 + for the transition metal ions and 2− for the oxygen ion, and up to 4000 neighboring ions were taken into account. Calculations were done for the substitutional site in the rutiles TiO_2, β-VO_2, GeO_2, RuO_2, and SnO_2; for the substitutional site and for an interstitial site in anatase TiO_2. For TiO_2, we choose $\langle r^2 \rangle$ and $\langle r^4 \rangle$ to fit our experimental results for the g tensor. For the other crystals (except RuO_2) we fitted $\langle r^2 \rangle$ and $\langle r^4 \rangle$ to published values[22–24] for g; in the case of RuO_2 we fitted them to the theoretical values for the ligand-field levels obtained from augmented-plane-wave and linear-combination-of-atomic-orbitals (APW-LCAO) calculations for reasons that will be discussed in Sec. V. The cell parameters and EPR data are given in Table I and the axes systems we use are defined in Fig. 1 for rutile and Fig. 2 for anatase. The fitted values for $\langle r^2 \rangle$ and $\langle r^4 \rangle$ are given in Table II. In all cases, the calculated and experimental values of Δg [see Eq. (1) below] agreed to better than 40%.

The rest of this paper will be restricted to a discussion of the TiO_2 results, unless otherwise noted. The eigen-

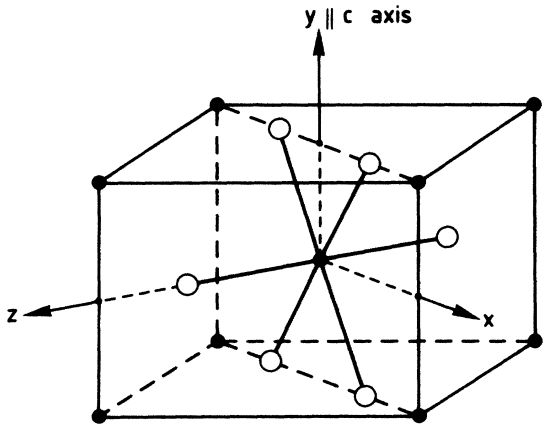

FIG. 1. Rutile primitive cell structure; the six oxygen anions (○) which are at the apexes of a distorted octahedron, give rise to an orthorhombic crystal field (D_{2h}) at the position of the metallic cation (●).

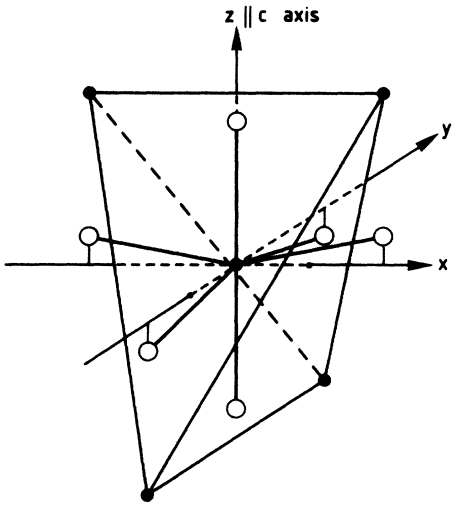

FIG. 2. Anatase cell structure; the six oxygen anions (○) which are at the apexes of a distorted tetrahedron, give rise to a tetragonal crystal field (D_{2d}) at the position of the metallic cation (●). The cell structure around the interstitial site is the same, except for the distances of the oxygens along z axis.

functions and eigenvalues of the full crystal-field Hamiltonian for a $3d_1$ electron centered at the substitutional site in rutile, the substitutional site in anatase, and the interstitial site in anatase are shown in Figs. 3, 4, and 5, respectively. When a vanadium ion is added in the lattice in an interstitial site, a charge compensation must arise in order to ensure the neutrality of the system. We have considered two mechanisms of compensation. (1) The four first titanium neighbors of the impurity which are lying in the x-y plane each take up one electron. (2) The four second titanium neighbors which are at the apexes of an elongated tetrahedron each take up one electron. The calculated values found in the second case fit better to the experimental data, but many other charge compensation schemes might do as well. It is important to note that the sequence of energy levels obtained when only the nearest neighbors are taken into account [Figs. 3(c) and 4(b)] is different from that obtained with 4000 neighbors [Figs. 3(b) and 4(a)]. For comparison, we have also considered two ligand-field-type models, that include covalent effects *a priori*: the angular overlap model, and the LCAO method. Both were restricted to nearest neighbors only. The angular overlap model[25] is generally considered as appropriate for weak covalent bonding. In our calculations for the substitutional site in rutile, we have introduced both π- and σ-antibonding effects, to lift the degeneracy of the levels completely, as required by the site symmetry. The level scheme we found is shown in Fig. 3(e). The model has been applied earlier[26] to fit the experimental values of a paramagnetic center attributed to substitutional Ti^{3+} in anatase. The result is reproduced in Fig. 4(d). LCAO calculations (restricted to the MO_6 cluster) for the substitutional sites in rutile and anatase have been reported by Grätzel and Rotzinger.[12] Their level schemes are shown in Figs. 3(d) and 4(c).

The deviations of the principal values of the g tensor from the free-spin value are given by second-order perturbation of the crystal-field levels by the spin-orbit and Zeeman interactions. Again as a result of covalency, the spin-orbit coupling constant in the real crystal will be

TABLE II. Radial averages $\langle r^2\rangle$, $\langle r^4\rangle$, and $\langle r^{-3}\rangle$ of the $3d_1$ orbital functions, orthorhombic mixing parameter α, spin-orbit constant λ, and g values of V^{4+} in the different host lattices. The g values, calculated on the basis of the parameters $\langle r^2\rangle$ and $\langle r^4\rangle$, are the best fit to the experimental data collected in Table I. In the case of RuO_2, we have given the values of $\langle r^2\rangle$ and $\langle r^4\rangle$ which permit our orbital energy levels to fit those found by APW-LCAO calculations (see Fig. 14 of Ref. 31). The free-ion values are based on Ref. 27. The experimental hyperfine constants introduced in Eq. (3) give $\langle r^{-3}\rangle$. The spin-orbit constant λ is equal to the free-ion value times the reduction factor (which is the ratio of the respective $\langle r^{-3}\rangle$ values).

	Free ion	TiO_2	β-VO_2	GeO_2	SnO_2	RuO_2	Anatase interstitial
$\langle r^2\rangle$ (Å^2)	$(0.62)^2$	$(0.93)^2$	$(1.2)^2$	$(0.8)^2$	$(1.2)^2$	$(1.1)^2$	$(0.53)^2$
$\langle r^4\rangle$ (Å^4)	$(0.73)^4$	$(1.24)^4$	$(1.3)^4$	$(1.15)^4$	$(1.4)^4$	$(1.15)^4$	1
$\langle r^{-3}\rangle$ (Å^{-3})	$(0.343)^{-3}$	$(0.386)^{-3}$	$(0.390)^{-3}$	$(0.396)^{-3}$	$(0.382)^{-3}$		$(0.378)^{-3}$
λ (cm^{-1})	255	179	173	165	184		189
α		0.049	0.029	0.014	0.107		0
g_x		1.911	1.928	1.905	1.946		1.96
g_y		1.915	1.962	1.939	1.893		1.96
g_z		1.959	1.972	1.956	1.965		1.932

smaller (by the orbital reduction factor k) than that of the free ion. The value of k can be obtained from the experimental hyperfine constants as will be described below [see Eq. (3)].

For the level schemes found in our 4000-ion crystal-field calculations, the values of the g tensor for the substitutional site in rutile are

$$\Delta g_x = c\frac{(1-\alpha\sqrt{3})^2}{E_{yz}} ,$$
$$\Delta g_y = c\frac{(1+\alpha\sqrt{3})^2}{E_{xz}} , \quad (1)$$
$$\Delta g_z = c\frac{4}{E_{xy}} ,$$

and for the interstitial site in anatase

$$\Delta g_x = 2k\lambda\frac{1}{E_{yz}} ,$$
$$\Delta g_y = 2k\lambda\frac{1}{E_{xz}} , \quad (2)$$
$$\Delta g_z = 8k\lambda\frac{1}{E_{x^2-y^2}} ,$$

where $c = 2k\lambda/(1+\alpha^2)$, the E_i are the covalent crystal orbital d energy levels, k is the reduction factor, λ is the spin-orbit constant of the free ion,[27] and α is the orthorhombic mixing coefficient. We find the ground orbital state in the substitutional site of anatase to be degenerated: therefore an EPR spectrum (if any) would be expected to be observable only at low temperatures.

The crystal-field levels found in Fig. 3(b) are also relevant to the spin relaxation results. All excited levels are high in energy compared to the Debye temperature. This implies specifically the impossibility of an Orbach relaxation process; and more generally that relaxation by phonon-induced crystal-field modulation will be relatively slow.

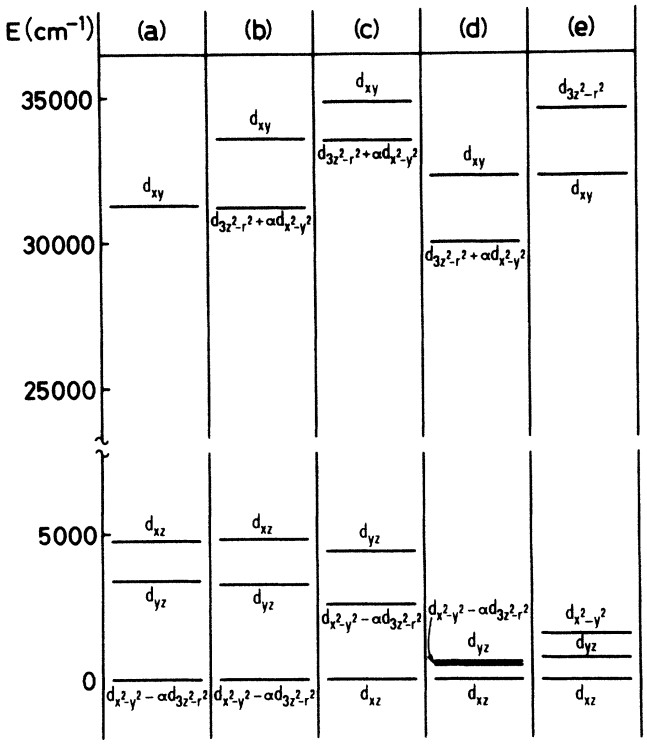

FIG. 3. $3d_1$ orbital energy levels of V^{4+} in the substitutional site of rutile TiO_2. α is the mixing parameter due to the orthorhombic symmetry. Its value is found to be 0.05. (a) Experimental values deduced from the g factors and the spin-orbit Hamiltonian. The ground level is assumed to be $d_{x^2-y^2}-\alpha d_{3z^2-r^2}$. (b) Calculated values with the point-charge model over 4000 ions. (c) Calculated values with the point-charge model, considering only the six nearest oxygen neighbors. (d) Results of the LCAO calculations reported in Ref. 12. (e) Calculated values with the angular overlap model, considering σ and π antibonding with the six nearest oxygens.

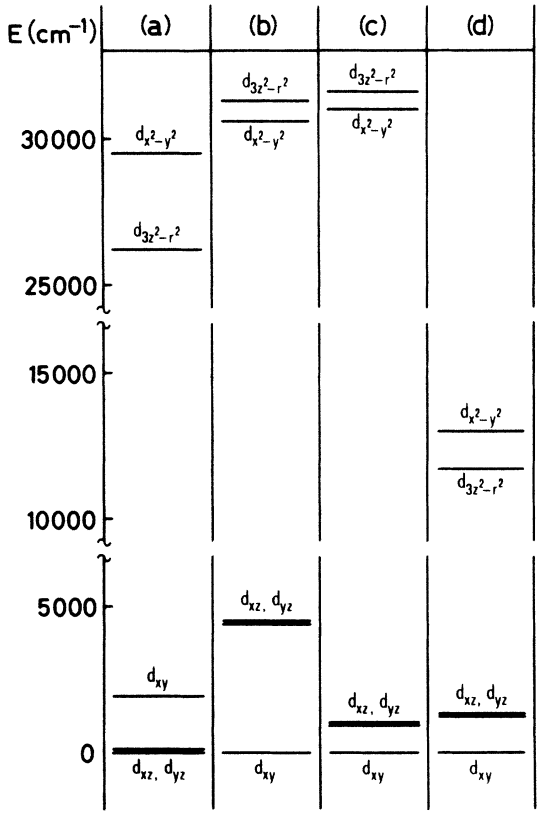

FIG. 4. $3d_1$ orbital energy levels of V^{4+} in the substitutional site of anatase TiO_2. (a) Calculated values with the point-charge model over 4000 ions. (b) Calculated values with the point-charge model, considering only the six first O^{2-} neighbors. (c) Results of the LCAO calculations reported in Ref. 12. (d) Results of the angular overlap model, from Ref. 26.

The magnetic hyperfine coupling is smaller than both the Zeeman and the spin-orbit interaction and is determined as a second-order perturbation of the ground level resulting from the crystal-field calculations. For ground levels of d_{xy}, $d_{x^2-y^2}$, and $d_{3z^2-r^2}$ types we find the dipolar hyperfine constant for the z direction to be given by

$$A_z^{\mathrm{dip}} = -\frac{\mu_0}{4\Pi} g_s g_n \mu_B \mu_n \langle r^{-3} \rangle \left[\frac{4}{7} \frac{1-\alpha^2}{1+\alpha^2} + \Delta g_z + \tfrac{3}{14}(\Delta g_x + \Delta g_y) - \tfrac{1}{3}(\Delta g_x + \Delta g_y + \Delta g_z) \right], \tag{3}$$

where μ_0 is the vacuum permeability, $g_s\mu_B$ the free-electron gyromagnetic ratio, μ_B the Bohr magneton, $g_n\mu_B$ the nuclear gyromagnetic ratio, μ_n the nuclear magneton, α the orthorhombic mixing coefficient, and $\langle r^{-3} \rangle$ the average value of r^{-3} over the ground orbital in the covalent crystal. The ratio of the value of $\langle r^{-3} \rangle$ found from Eq. (3) to that in the free ion gives the orbital reduction factor k. The results are shown in Table II.

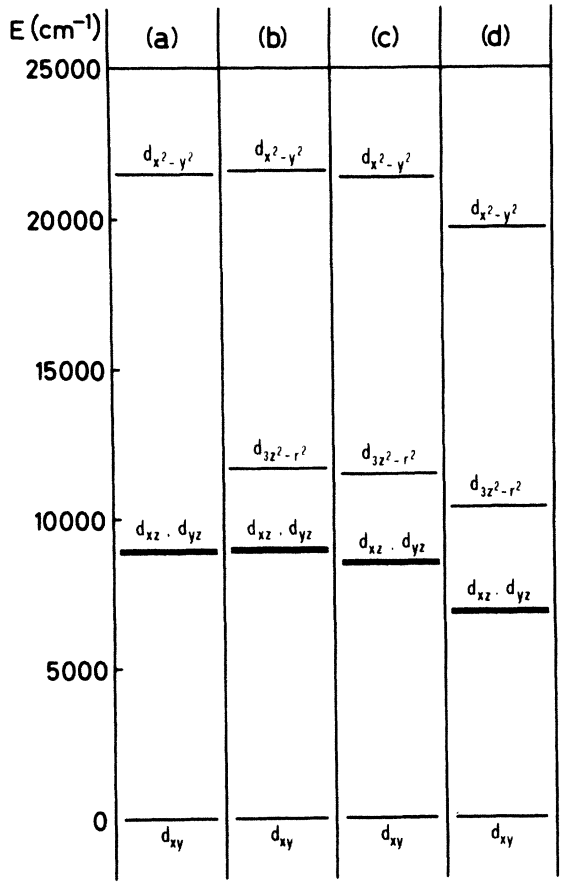

FIG. 5. $3d_1$ energy levels of V^{4+} in the interstitial site of anatase. Experimental and point-charge model determinations. (a) Experimental values deduced from the spin-orbit coupling. (b) Calculations with a charge compensation on the four second titanium neighbors of the impurity which are positioned at the apexes of a elongate tetrahedron. (c) Calculations without any charge compensations. (d) Calculations with a charge compensation on the four first titanum neighbors of the impurity which are lying in the x-y plane.

IV. EPR RESULTS

We have observed the X-band EPR spectrum of V^{4+} in rutile in the single crystal, in a powder obtained by grinding part of the crystal, and in several powders prepared from the sol, at temperatures between 4.2 and 300 K. Parameters of the powder spectra were derived from comparison of experimental and calculated spectra. The best fit was obtained using the parameters also found from the single-crystal spectra, given in Table I, that are in good agreement with earlier results.[10,11] In the single-crystal case at low temperature we found the superhyperfine coupling of about 1 G to nearest-neighbor Ti that has been reported earlier.[19–21] Linewidths in the single crystal at low temperatures were well below 1 G, less than in a previous study.[5] In the three kinds of rutile samples, we have measured T_1 of the highest-field hyperfine line between 4.2 and 77 K by pulse methods (see Fig. 6). Results on the

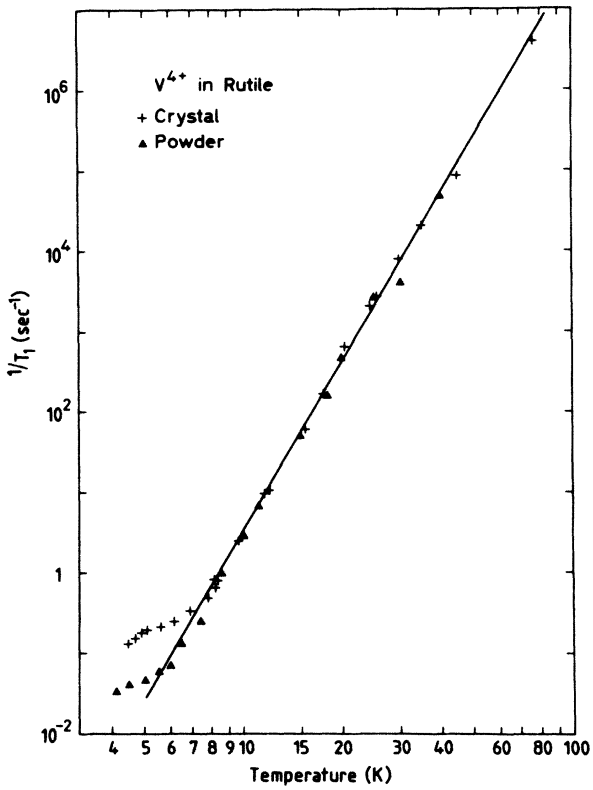

FIG. 6. Temperature dependency of the spin-lattice relaxation time T_1 of V^{4+} in the substitutional site of TiO_2 rutile, measured in the highest hyperfine line at 9.3 GHz. +, single-crystal case, with the magnetic field along [0,0,1]. V^{4+} concentration 0.02%. ▲, powder case, V^{4+} concentration 0.01%. The straight line represents a T^7 temperature variation. A powder prepared from the single crystal gives the same result as the crystal.

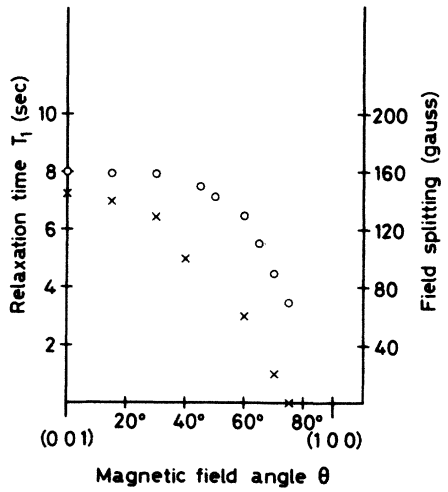

FIG. 7. ×, angular dependency of the spin-lattice relaxation time T_1 of V^{4+} in the substitutional site of TiO_2 rutile single crystal, measured in the highest hyperfine line ○, angular dependency of the magnetic field separation with the nearest hyperfine line. The concentration of V^{4+} is 0.02%. The spin-lattice relaxation time has been measured at 4.2 K.

single crystal and on the powder prepared from it were the same. At 4.2 and 18 K we studied the field and frequency dependence of the relaxation time. At constant frequency, we found no difference between the lowest- and highest-field hyperfine lines (the intermediate lines relax faster, due to overlap). No variation of T_1 of the high-field line was found for microwave frequencies between 8 and 11 GHz. In the single crystal at 4.2 K we found an orientation dependence as shown in Fig. 7. It is seen that the relaxation becomes faster when the hyperfine line splitting decreases. The data at higher temperatures

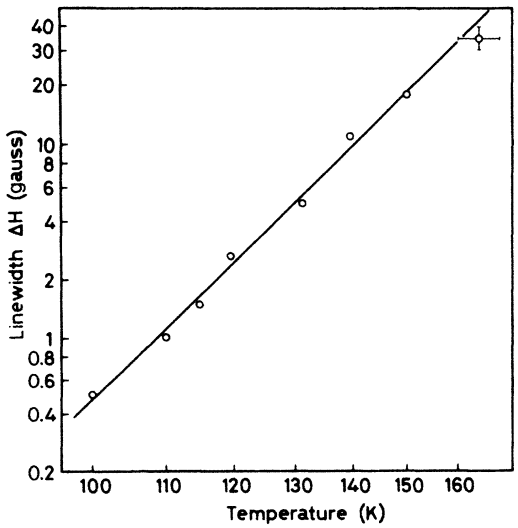

FIG. 8. Temperature dependency of the highest hyperfine linewidth of V^{4+} in the single crystal of TiO_2 rutile. It may be fitted with a T^9 process. The field is along the c axis. The V^{4+} concentration is 0.02%.

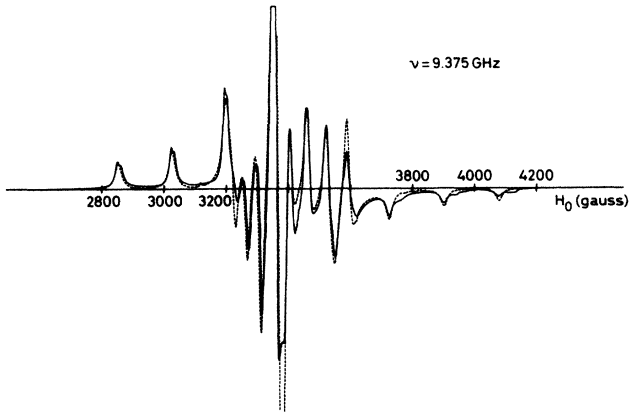

FIG. 9. EPR powder spectrum of V^{4+} in the interstitial site of anatase experimental (——) and numerical simulation (— — —).

(see Fig. 6) are concentration independent and vary with temperature as T^7 over several decades. At low temperatures the variation is approximately as T^1 over a range of a factor of 3; but here T_1 varies with concentration.

In Fig. 8 we have plotted the linewidth of the highest-field hyperfine line in the single crystal as a function of temperature. It fits very well to a T^9 variation over an order of magnitude.

The anatase has been studied by cw ESR in powder and in a colloid. In both cases the size of the particles is very small (about 200 Å). From 4.2 to 300 K, the same spectrum, shown in Fig. 9, has been observed corresponding to $S=\frac{1}{2}$ and $I=\frac{7}{2}$. There is no line broadening with increasing temperature. Powder spectra have also been observed at the K band. The EPR parameters have been obtained by fitting simulated spectra to the observed spectra. Because of the small size of the anatase powder (200 Å diameter), the inhomogeneous linewidth is important. The convolution with a Lorentzian line shape of width 25 G leads to a good fit of the experimental spectrum, as shown in Fig. 9, with the parameters listed in Table I.

The spin-lattice relaxation time measured from 4.2 to 77 K for three powdered samples of anatase with different nominal concentrations of vanadium are shown in Fig. 10. As in the case of rutile, the relaxation curves observed at low temperature vary with concentration. At high temperatures, the temperature variation follows a power law with exponent 5.7. As mentioned above, no line broadening (beyond the value of 25 G used in the fit) is found up to 300 K.

V. DISCUSSION

In rutile, g_x and g_y differ only by 0.1%. This has been taken as an indication of a very nearly tetragonal distortion,[11] so that Abragam and Pryce's theory[28–30] should be applicable; but when this is done, the results are disappointing.[11] In the Abragam and Pryce approximation, values of $g_{\|}$ and $g_{\perp}$ are deduced by exact simultaneous diagonalization of the tetragonal crystal field and the spin-

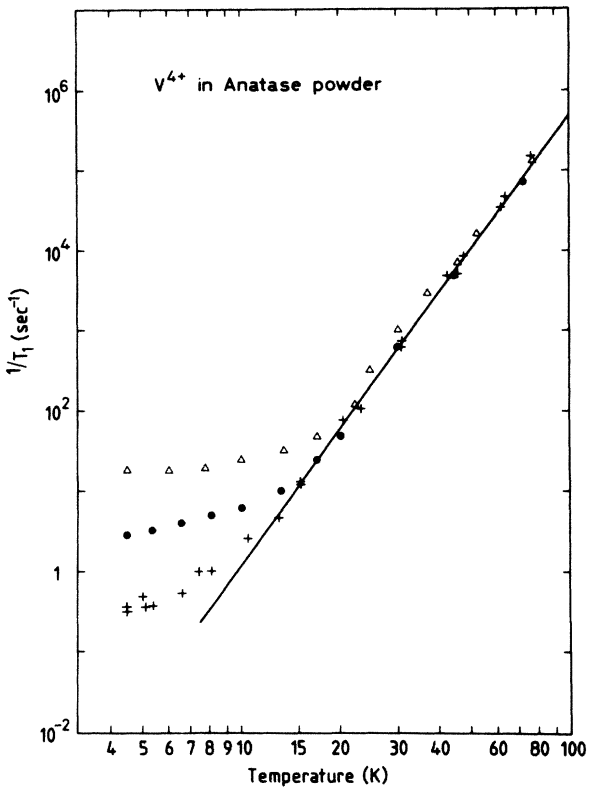

FIG. 10. Temperature dependency of the spin-lattice relaxation time T_1 of V^{4+} in the interstitial site of anatase. Three impurity's concentrations: 0.01% (+), 0.05% (●), and 0.5% (△) are considered ($\nu=9.3$ GHz).

orbit operators within the lower orbital triplet due to the cubic crystal field, ignoring all couplings to the upper doublet. It is easy to show from Eq. (1), that in orthorhombic symmetry g_x may be very close (or even equal) in value to g_y, while the mixing parameter α remains very different from zero, so that Abragam and Pryce's approximation is not applicable. When the theory is applied to anatase, poor results are obtained, even though the symmetry is tetragonal. This is due to the presence of higher-order terms in a perturbation treatment of the spin-orbit interaction, that connect the ground state to the upper doublet. These terms become important when the tetragonal splitting is not very weak with respect to the cubic one.

Therefore the level scheme resulting from the complete crystal-field Hamiltonian, as in Figs. 3–5, has to be used in both rutile and anatase as the starting point for determining the EPR parameters. From inspection of Figs. 3 and 4, it will be seen that the nearest-neighbor-only results from point charge, angular overlap, and LCAO calculations for the substitutional sites all give the same ground state: d_{xz} for rutile and d_{xy} for anatase. The 4000-neighbor point-charge model, on the other hand, gives a mixture of $d_{x^2-y^2}$ with $d_{3z^2-r^2}$ for rutile, and degenerate d_{xz} and d_{yz} for anatase. The experimental values for the g and A tensors in rutile can be brought into good agreement with Eqs. (1) and (3) valid for $d_{x^2-y^2}$, $d_{3z^2-r^2}$, and d_{xy} ground states, but *not* with the corresponding equations for a d_{xz} ground state. So if we assume the V^{4+} to be in a substitutional site in rutile, then the crystal-field (ligand-field) levels found in any of the nearest-neighbor-only models must be wrong, but those of the 4000-neighbor point-charge calculations may be right.

To test the reliability of our simple point-charge calculation scheme, we have applied it to RuO_2, where ligand-field levels have been obtained from an APW-LCAO band-structure calculation by Mattheiss.[31] For any reasonable value of the parameter $\langle r^2\rangle$ and $\langle r^4\rangle$ we obtain the same level sequence as given in Fig. 14 of Ref. 31. The best agreement is found with the values given in Table II. Since the 4000 point-charge model agrees so well with both the more sophisticated calculation and the experimental result in rutile, we feel it must be superior to the nearest-neighbor-only result in anatase as well. If this is the case, then the EPR signal of V^{4+} (or Ti^{3+}) in anatase cannot be due to ions in a substitutional site.

Meriaudeau and Vedrine[32] have reported that V^{4+} ions detected by electron spectroscopy for chemical analysis in anatase powders could not be found by EPR. They proposed that the vanadium ions are contained in small regions of V_2O_4 and do not give an EPR signal. This assumption is not necessary: if the ions are simply substituting for Ti^{4+} in anatase, they cannot be observed by EPR either. A number of results is available for the isoelectronic Ti^{3+} in anatase. Meriaudeau *et al.*[26] have found a signal with $g_{\|}=1.959$ and $g_{\perp}=1.990$, and on the basis of the angular overlap model attributed it to substitutional Ti^{3+} [see Fig. 4(d)]. Recently, Howe and Grätzel[13] have observed the same signal ($g_{\|}=1.957$ and $g_{\perp}=1.988$), but they attributed it to an interstitial Ti^{3+} ion. The free Ti^{3+} ion has a weaker spin-orbit coupling (by a factor of 0.6) and larger $\langle r^2\rangle$ and $\langle r^4\rangle$ values (by a factor of 1.17^2 and 1.18^4) than the free V^{4+}. From our data for V^{4+} in anatase (Tables I and II) and from Eq. (2) we therefore expect Ti^{3+} in the interstitial site to have $1.984<g_x=g_y<1.989$ and $g_z=1.981$. The poor agreement of g_z with the experimental results for Ti^{3+} probably indicates that the charge compensation mechanisms are different in the two systems. Howe and Grätzel[13] have also reported that the signal of Ti^{3+} obtained by uv-irradiation is stable only at low temperature. The intensity of the V^{4+} signal that we have observed does not vary with time, even at room temperature. Charge migration apparently is more important in the case of Ti^{3+}, again pointing to a different charge compensation mechanism. The expected g values for Ti^{3+} in the substitutional site of rutile deduced from those of V^{4+} are $1.963<g_x=g_y<1.975$ and $1.982<g_z<1.988$; here again the charge compensation of Ti^{3+} may be involved to explain $g_z=1.941$ observed by Chester.[33]

After converting the anatase powders to rutile by heating in air to 700°C, the V^{4+} ions are found at substitutional sites. This is similar to what has been observed in single crystals of rutile:[34] in the fully oxidized state, the vanadium ions are substitutional; in the slightly reduced state they are interstitial, and after heavy reduction nonmagnetic V^{3+} is obtained. It seems therefore likely that our anatase powders are slightly reduced. The undoped

powders have been found to behave as n-type semiconductors:[2] these properties might be due to interstitial Ti^{3+} occurring in slightly reduced material.

Let us now turn to the spin-relaxation in rutile. Going from low to high temperatures, the exponent of its temperature variation changes from 1 to 7 to 9. An exponent of 1 is a characteristic of the "direct process," that has been proposed as the low-temperature relaxation mechanism in earlier work.[5] The values we obtain are concentration dependent, larger by a factor of 10 than those found by Sanders and Rowan,[35] larger by a factor of 200 than those measured by Chingas and Rowan,[36] and larger by a factor of 20 than those of Zverev.[5] Furthermore, we have not found the characteristic H^2 dependence nor the $\sin(2\theta)$ angular variation of the direct process. We therefore propose that these long values of T_1 are due to cross relaxation to other, unidentified, paramagnetic impurities; for such a mechanism of course, the size effect expected[6] for the "direct process" need not be present.

For a Kramers ion, the temperature exponent 7 for T_1 is very unusual. It could theoretically arise from symmetry breaking by the magnetic field, in which case a H^2 field dependence should occur. We have not found such a dependence. Now, although couplings to the crystal field are generally thought to be more effective in producing relaxation than spin-spin interactions, exceptions to the rule do occur when the coupling to the crystal field is very weak, as in the case of F centers.[37,38] When we extrapolate the linewidth data of Fig. 8, that do show the usual Kramers ion T^9 variation, to the lower-temperature range, fairly long relaxation times from this mechanism are predicted. We take this as an indication that the T^7 variation is not due to the crystal field together with some particular phonon spectrum that cuts the expected exponent by two units, but rather to some spin-spin interaction; specifically the hyperfine coupling. As a starting point in estimating the efficiency of such a mechanism, we show in Fig. 11 the relation between $\langle r^{-3} \rangle$ as derived from Eq. (3) and the inverse of the third power of the mean metal-ion—oxygen-ion distance, as given in Table I for different rutile-type crystals. The extrapolation of these data on the plot to infinite distance approximates very well the value of $\langle r^{-3} \rangle$ calculated for the free ion.[27] Therefore we deduce that modulation of the Ti-O distance by the phonons will lead to a corresponding modulation of $\langle r^{-3} \rangle$ for the $3d_1$ wave function, and therefore of the hyperfine coupling [see Eq. (3)]. Although a full calculation of the relaxation time is complicated (and will not be very reliable) it should be noted that for spin-spin interactions the "anharmonic Raman process" is expected to be several orders of magnitude more efficient[39] than the "harmonic Raman process" (the only one operative in relaxation by crystal-field modulation). We estimate that relaxation times of the order of 1 s at 10 K can be obtained by this process for V^{4+} in rutile.

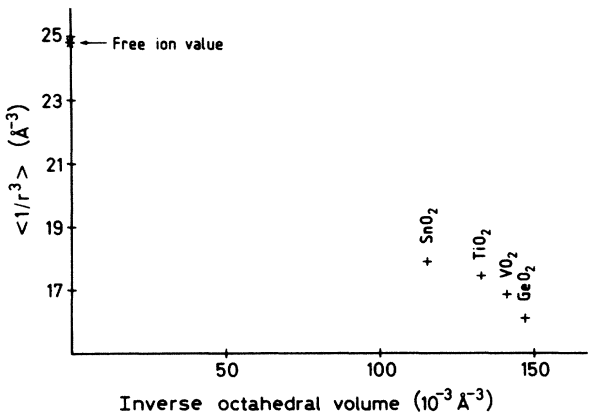

FIG. 11. Average value of the substitutional V^{4+} $3d_1$ electron radial function r^{-3} in different rutile-type crystals as a function of the surrounding oxygen distorted octahedron volume.$^{-1}$

Above 100 K, the linewidth increases as T^9 with temperature, characteristic of Raman relaxation through coupling with the crystal field for a Kramers ion. Previously, an Orbach process to an excited state at 650 cm^{-1} has been proposed[5] in this temperature region; but our calculations (see Fig. 3) show that it is unlikely that such a state exists (judging from the figures in Ref. 5 it seems that those data would fit a T^9 law equally well).

So far, we have not been able to identify properly the relaxation mechanism in anatase. It seems to be slower still than that in rutile (see Fig. 10); the unusual exponent may be related to the V^{4+} ion's being interstitial.

VI. SUMMARY

The sequence of orbital energy levels of a $3d_1$ electron at the metal ion site in the rutile structure can be calculated from a relatively simple point-charge model, subject to the condition that a sufficient number of ions is considered. For comparison to experimental EPR data, two parameters of the model, $\langle r^2 \rangle$ and $\langle r^4 \rangle$, must be adjusted: reasonable values are obtained for the four crystals considered. When only nearest-neighbor oxygen ions are taken into account, all three models considered (point charges, angular overlap, LCAO) give erroneous results for rutile. We therefore suppose that the many-neighbor point-charge model should also yield the correct level sequence in the anatase structure. If this is correct, the EPR signals from V^{4+} and Ti^{3+} in anatase powders must be due to ions in an interstitial site.

The level spacing in rutile also shows that spin relaxation by the Orbach process is impossible. We show experimentally that the process previously identified as an Orbach one is the normal Raman relaxation by crystal-field modulation of a Kramers ion. Similarly, our experiments show that at low temperatures there is no "direct" relaxation process (contrary to what has been reported earlier) so that rutile and anatase powders are not suitable candidates to look for a "size effect" in spin relaxation. In an intermediate-temperature range we believe the relaxation occurs through hyperfine coupling,[37,38] which is rather unusual for transition-metal ions and contrary to what has been suggested.[10] Thus, the dynamical coupling of these Kramers ions to the crystal field is weak, and relaxation times are relatively long.

ACKNOWLEDGMENTS

The authors gratefully acknowledge the help of C. K. Jørgensen for his comments on the angular-overlap model and F. P. Rotzinger for many helpful discussions on the LCAO model. It is a pleasure to thank A. Châtelain for his contributions.

[1]F. Gervais and W. Kress, Phys. Rev. B **28**, 2962 (1983).
[2]C. N. R. Rao and G. V. Subba Rao, *Transition Metal Oxides,* Natl. Bur. Stand. Ref. Data Ser., Natl. Bur. Stand. (U.S.) (U.S. GPO, Washington, D.C., 1974).
[3]K. Kalyanasundaram, M. Grätzel, and E. Pelizzetti, Coord. Chem. Rev. **69**, 57 (1986).
[4]V. S. Grunin, V. A. Ioffe, I. V. Patrina, and G. D. Davtyan, Fiz. Tverd. Tela (Leningrad) **17**, 3034 (1975) [Sov. Phys.—Solid State **17**, 2012 (1976)].
[5]G. M. Zverev, Zh. Eksp. Teor. Fiz. **44**, 1859 (1963) [Sov. Phys.—JETP **17**, 1251 (1963)].
[6]A. M. Stoneham, Solid State Commun. **3**, 71 (1965).
[7]J. Moser and M. Grätzel, J. Am. Chem. Soc. **105**, 6547 (1983).
[8]T. Shimizu, J. Phys. Soc. Jpn. **23**, 848 (1967).
[9]G. J. Hyland, J. Phys. C **1**, 189 (1968).
[10]G. M. Zverev and A. M. Prokhorov, Zh. Eksp. Teor. Fiz. **39**, 222 (1960) [Sov. Phys.—JETP **12**, 160 (1960)].
[11]H. J. Gerritsen and H. R. Lewis, Phys. Rev. **119**, 1010 (1960).
[12]M. Grätzel and F. P. Rotzinger, Chem. Phys. Lett. **118**, 474 (1985).
[13]R. F. Howe and M. Grätzel, J. Phys. Chem. **89**, 4495 (1985).
[14]J. Moser and M. Grätzel, Helv. Chim. Acta **65**, 1436 (1982).
[15]We thank Dr. R. Humphry-Baker for performing light-scattering experiments for particle-size determination.
[16]R. Gallay and J. J. van der Klink, J. Phys. E **19**, 226 (1986).
[17]E. L. Hahn, Phys. Rev. **80**, 580 (1950).
[18]M. T. Hutchings, in *Solid State Physics,* edited by H. Ehrenreich, F. Seitz, and D. Turnbull (Academic, New York, 1964), Vol. 16, p. 227.
[19]D. P. Madacsi, M. Stapelbroek, R. B. Bossoli, and O. R. Gilliam, J. Chem. Phys. **77**, 3803 (1982).
[20]E. Yamaka and R. G. Barnes, Phys. Rev. A **135**, 144 (1964).
[21]F. C. Newman and L. G. Rowan, Phys. Rev. B **5**, 4231 (1972).
[22]I. Siegel, Phys. Rev. A **134**, 193 (1964).
[23]C. Kikuchi, I. Chen. W. H. From, and P. B. Dorain, J. Chem. Phys. **42**, 181 (1965).
[24]J. Umeda, H. Kusumoto, and N. Narita, Proceedings of the International Conference on the Physics of Semiconductors, Kyoto (1966) [J. Phys. Soc. Jpn. Suppl. **21**, 619 (1966)].
[25]C. K. Jørgensen, J. Phys. (Paris) **26**, 825 (1965).
[26]P. Meriaudeau, M. Che, and C. K. Jørgensen, Chem. Phys. Lett. **5**, 131 (1970).
[27]Table 7.6, p. 399, in *Electron Paramagnetic Resonance of Transition Ions,* edited by A. Abragam and B. Bleaney (Clarendon, Oxford, 1970).
[28]B. Bleaney, Proc. Phys. Soc. **63**, 407 (1950).
[29]A. Abragam and M. H. L. Pryce, Proc. R. Soc. London, Ser. A **205**, 135 (1951).
[30]D. K. Réi, Fiz. Tverd. Tela (Leningrad **3**, 15 (1961) [Sov. Phys.—Solid State **3**, 1845 (1962)].
[31]L. F. Mattheiss, Phys. Rev. B **13**, 2433 (1976).
[32]P. Meriaudeau and J. C. Vedrine, Nuov. J. Chim. **2**, 133 (1977).
[33]P. F. Chester, J. Appl. Phys. Suppl. **32**, 2233 (1961).
[34]F. Kubec and Z. Šroubek, J. Chem. Phys. **57**, 1660 (1972).
[35]R. L. Sanders and L. G. Rowan, Phys. Rev. Lett. **21**, 140 (1968).
[36]G. Chingas and L. G. Rowan, Phys. Rev. B **27**, 2636 (1983).
[37]V. Ya. Kravchenko and V. L. Vinetskii [Sov. Phys.—Solid State **6**, 1638 (1965)]. Fiz. Tverd. Tela (Leningrad) **6**, 2075 (1965).
[38]V. Ya. Kravchenko and V. L. Vinetskii [Sov. Phys.—Solid State **7**, 1 (1965)]. Fiz. Tverd. Tela (Leningrad) **7**, 3 (1965).
[39]J. van Kranendonk and M. B. Walker, Can. J. Phys. **46**, 2441 (1968).
[40]*Gmelins Handbuch der Anorganischen Chemie,* 8th ed. (Verlag Chemie, Weinheim, 1951).
[41]D. T. Cromer and K. Herrington, J. Am. Chem. Soc. **77**, 4708 (1955).